Evidence for the charge-density-wave nature of the stripe phase in manganites

2007 J. Phys.: Condens. Matter 19 192201

(http://iopscience.iop.org/0953-8984/19/19/192201)

IOP FTC

IOP PUBLISHING JOURNAL OF PHYSICS: CONDENSED MATTER

J. Phys.: Condens. Matter **19** (2007) 192201 (7pp) doi:10.1088/0953-8984/19/19/192201

FAST TRACK COMMUNICATION

Evidence for the charge-density-wave nature of the stripe phase in manganites

S Cox[1,2], J C Lashley[3], E Rosten[3], J Singleton[1], A J Williams[4] and P B Littlewood[5]

[1] National High Magnetic Field Laboratory, Los Alamos National Laboratory, Ms-E536, Los Alamos, NM 87545, USA
[2] Department of Materials Science and Metallurgy, University of Cambridge, Cambridge CB2 3QZ, UK
[3] Los Alamos National Laboratory, Los Alamos, NM 87545, USA
[4] Centre for Science at Extreme Conditions, University of Edinburgh, Edinburgh EH9 3JZ, UK
[5] Cavendish Laboratory, University of Cambridge, Cambridge CB3 0HE, UK

Received 22 March 2007
Published 26 April 2007
Online at stacks.iop.org/JPhysCM/19/192201

Abstract

Heat capacity and magnetization measurements strongly suggest that the onset of the stripe phase in $La_{0.50}Ca_{0.50}MnO_3$, $La_{0.48}Ca_{0.52}MnO_3$ and $Pr_{0.48}Ca_{0.52}MnO_3$ is due to the formation of a charge density wave. The transition associated with the onset of the stripe phase is second order, and it can be well modelled as a Peierls transition (typically associated with charge-density-wave formation) in a disordered system (a 'dirty' Peierls transition). The entropy change at this transition is very similar for $La_{0.50}Ca_{0.50}MnO_3$, $La_{0.48}Ca_{0.52}MnO_3$ and $Pr_{0.48}Ca_{0.52}MnO_3$, suggesting a common origin. We show that this is not associated primarily with magnetic order since the magnetization varies by a factor of 100 between the compositions while the change in entropy remains roughly constant.

(Some figures in this article are in colour only in the electronic version)

Many strongly correlated electron systems (e.g., manganites [1, 2], cuprates [3], nickelates [4] and cobaltites [5]) exhibit stripe phases, in which a superstructure forms at low temperatures. The results of transmission electron microscopy (TEM) [1, 2, 6] and neutron diffraction [7, 8] experiments in the manganites led to the suggestion that the superstructure formation was driven by charge separation and localization at atomic sites. However, the interpretation of the high-resolution TEM results has been challenged [9], and more recent experiments with the same technique on layered manganites indicated a smoothly varying superstructure [10]. Recent work has produced conflicting evidence as to the nature of the superstructure, with some studies supporting a model with charge localized at the atomic sites, but with the difference in charge between atomic sites being small [11–15], and others indicating that the superstructure is not tied to the atomic sites [16, 17]. To explain the latter results, it has been proposed that the superstructure resembles a charge density wave (CDW) [10, 16, 18]. In this paper, we show

Table 1. Average and variance of the radius of the site occupied by rare earth (Re) or alkaline earth (Ae) ions in different compositions of $Re_{1-x}Ae_xMnO_3$ (the Re/Ae site radius). Here Re is La or Pr, Ae is Ca and $x = 0.5$ or 0.52 [24].

	Average Re/Ae site radius (Å)	Variance of Re/Ae site radius (Å^2)
$La_{0.50}Ca_{0.50}MnO_3$	1.198	3.24×10^{-4}
$La_{0.48}Ca_{0.52}MnO_3$	1.197	3.23×10^{-4}
$Pr_{0.48}Ca_{0.52}MnO_3$	1.180	2.50×10^{-7}

that heat capacity measurements provide strong support for a CDW model of the superstructure in manganites.

Previous thermal measurements of $La_{1-x}Ca_xMnO_3$ with $x \geqslant 0.5$ [19–22] have observed two transitions as peaks in the heat capacity when plotted as a function of temperature (T). The peak at higher T was attributed to order–disorder-type critical fluctuations [19, 20], with a contribution at $x = 0.5$ from the onset of ferromagnetism (FM). The transition was identified as first order, based on the hysteresis in the resistivity data [21]. The lower T peak was attributed to the transition from a ferromagnetic state to an antiferromagnetism (AFM) [19–22]. Here we use heat capacity and magnetization measurements to gain insight into the nature of these phase transitions. Measurements were made on $La_{0.50}Ca_{0.50}MnO_3$, $La_{0.48}Ca_{0.52}MnO_3$ and $Pr_{0.48}Ca_{0.52}MnO_3$, with the latter two being chosen as compounds with different average cation sizes and variances (see table 1) but in which the superstructure has on average an almost identical wavevector present in all grains, as measured by TEM and neutron diffraction [17]. Since the superstructure is present in all grains with a similar wavevector, it is appropriate to model the system macroscopically as a single ordered phase. The smaller size of the Pr cation is thought to lead to stronger electron–phonon coupling, allowing the superstructure to lock into the lattice in around 25% of the grains [17]. The $La_{0.50}Ca_{0.50}MnO_3$ sample was chosen as it has a nominally commensurate superstructure (though small deviations are seen in TEM measurements [23]) and so provides a contrast between commensurate and incommensurate systems.

Samples were prepared by repeated grinding, pressing and sintering of appropriate oxides and carbonates in stoichiometric proportions. The carbonates were decarboxylated by heating for 12 h at 950 °C. Each sample was twice reground, repelleted and heated at 1350 °C for 4 days. X-ray powder diffraction indicated that the samples were single phase [25]. Heat capacity measurements were made using a Quantum Design Physical Properties Measurement System (PPMS). In order to ensure that the system had reached equilibrium the heat capacity measurements were taken with very dense data points, with a 20 min pause at each T (decreasing the period to 3 min produced substantially different data at of the transitions). The long relaxation times at each T hints at pinning of the superstructure to defects in the system [26]. Magnetic susceptibility measurements were performed using a Quantum Design MPMS. Samples masses were between 30 and 45 mg.

The heat capacity data for all three compounds show two transitions (see figure 1), with the transition at higher T exhibiting a much larger change in entropy than the lower transition. In order to make the transitions more visible the background was removed from the data. In the low T (1.8–10 K) range, heat capacity data were fitted to an equation of the form

$$C_P = \beta_3 T^3 + \beta_5 T^5 + \gamma T + \frac{\alpha}{T^2} + \delta T^2, \tag{1}$$

where β_3, β_5, α, δ and γ are constants; $\beta_3 = Nk\frac{12\pi^4}{5}\frac{1}{\theta_D^3}$, where θ_D is the Debye T. The high T data are modelled with a Debye model and an Einstein mode, where θ_D has been determined

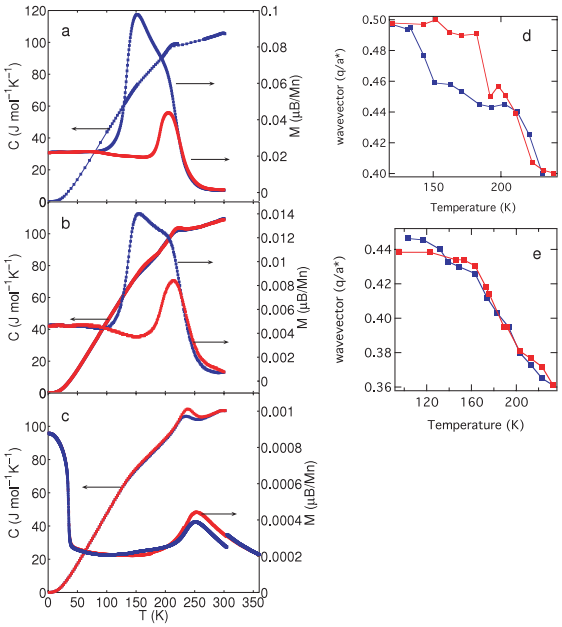

Figure 1. Heat capacity, and magnetization (in 100 Oe), with warming data shown in light grey/red and cooling data shown in dark grey/blue. (a) shows data for $La_{0.50}Ca_{0.50}MnO_3$, (b) shows data for $La_{0.48}Ca_{0.52}MnO_3$, and (c) shows data for $Pr_{0.48}Ca_{0.52}MnO_3$. The errors are smaller than the size of the data points. The variation of the wavevector of the superstructure wavevector with T is shown for $La_{0.50}Ca_{0.50}MnO_3$ in (d) (data from [6]) and for $La_{0.48}Ca_{0.52}MnO_3$ in (e) (data from [16]).

from the low T data. The data were fitted with iterative reweighted least squares using the Levenberg–Marquardt method [27]. This method has the advantage over the more commonly used least-squares technique that low weights are automatically given to areas which have a poor fit to the model (so the errors are not assumed to be Gaussian). The heat capacity above background is shown in figures 2(a)–(c).

As can be seen from figures 1(d), (e), 2(a) and (b) the appearance of the superlattice reflections occurs at the same T as the upper transition, and the stabilization of the value of the wavevector occurs at the same T as the lower transition. This indicates that the evolution of the superstructure is strongly linked to the phase transitions. The hysteresis observed in the heat capacity data cannot be taken as evidence for a first-order transition. Similar hysteresis is observed in the impurity-pinned CDW transition in $Lu_5Rh_4Si_{10}$ [28]. The transition to the CDW state in $Lu_5Rh_4Si_{10}$ is unambiguously second order [28]; below we shall demonstrate that the transitions to the manganite superstructure states shown in figure 1 are also second order and CDW like.

The magnetization data for $La_{0.50}Ca_{0.50}MnO_3$ and $La_{0.48}Ca_{0.52}MnO_3$ show an increase in moment on cooling corresponding to a transition of some proportion of the sample to FM (figure 1). At lower Ts the magnetization falls again—this is traditionally associated with the transition to AFM [29]. In the T range between the two transitions, hysteresis is observed in M–H loops (figure 3).

The presence of an FM–AFM transition in $La_{0.50}Ca_{0.50}MnO_3$ and $La_{0.48}Ca_{0.52}MnO_3$ agrees with the suggestion of Milward *et al* [18] that the superstructure of a stripe phase which has not locked into its low T value will always be associated with ferromagnetism. The magnetization is higher for $La_{0.50}Ca_{0.50}MnO_3$ than for $La_{0.48}Ca_{0.52}MnO_3$, as predicted by Landau theory [18].

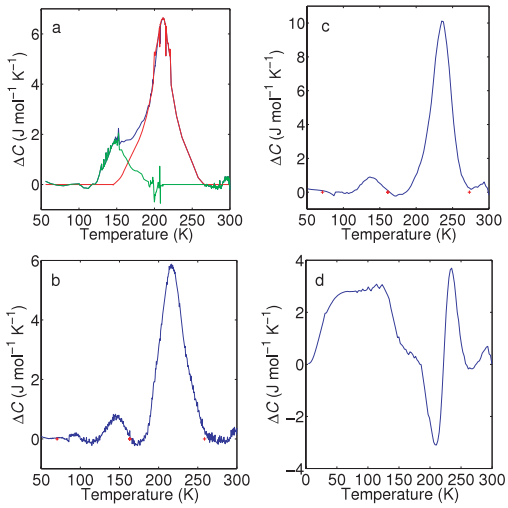

Figure 2. Excess heat capacity of (a) $La_{0.50}Ca_{0.50}MnO_3$, (b) $La_{0.48}Ca_{0.52}MnO_3$ and (c) $Pr_{0.48}Ca_{0.52}MnO_3$ with background removed. (d) $La_{0.48}Ca_{0.52}MnO_3$ heat capacity subtracted from $Pr_{0.48}Ca_{0.52}MnO_3$ heat capacity. In (a) the dark grey/blue line is total heat capacity above background. The light grey/red and green lines show the contributions of the upper and lower T transitions respectively. In (b) and (c) the (red) crosses signify the limits used for the entropy calculation.

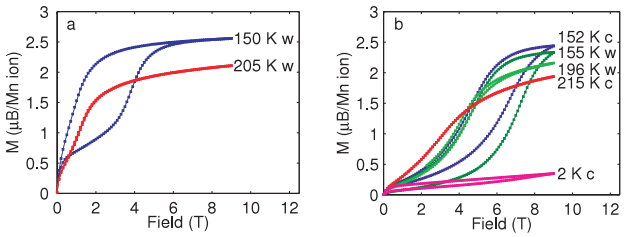

Figure 3. M–H loops taken at various Ts on warming and cooling for (a) $La_{0.50}Ca_{0.50}MnO_3$ and (b) $La_{0.48}Ca_{0.52}MnO_3$. Curves were taken on warming (w) and cooling (c).

The magnetization for $Pr_{0.48}Ca_{0.52}MnO_3$ shows a change in the region of the transitions that is only 1% of that for $La_{0.50}Ca_{0.50}MnO_3$, and a marked increase in moment below 50 K, where there are no features in the heat capacity data. However, the $La_{0.48}Ca_{0.52}MnO_3$ and $Pr_{0.48}Ca_{0.52}MnO_3$ heat capacity data show a constant difference (average 8%) in the range 20–100 K (figure 2), with an extra entropy of 5.1 J mol^{-1} K^{-1} arising in $Pr_{0.48}Ca_{0.52}MnO_3$ relative to $La_{0.48}Ca_{0.52}MnO_3$ in this T range. Since the masses of Pr and La differ by only 1.4%, the change in the phonon contribution to the heat capacity is unlikely to have produced the large observed difference [30]. Thus there may be a magnetic phase in $Pr_{0.48}Ca_{0.52}MnO_3$ which evolves continuously between 2 and 50 K.

The calculated entropies (see table 2) are lower by a factor of around two than those found in other studies of similar compounds [22, 31]. This difference is probably due to the fact that the entropies in [22, 31] were calculated by fitting a polynomial away from the region of the transitions, rather than using all of the data to fit a background which is smooth in the region of the transitions, as done in the present work.

We now show that the two transitions are dominated by electron–lattice effects associated with the superstructure. The entropy released at the higher temperature transition is similar

Table 2. Entropy values for the transition to the stripe phase in various manganite compounds.

	S of lower transition		S of upper transition		
	J mol^{-1} K^{-1}	% of S_{tot}	J mol^{-1} K^{-1}	% of S_{tot}	References
$La_{0.50}Ca_{0.50}MnO_3$	0.41	24	1.33	76	This work
$La_{0.48}Ca_{0.52}MnO_3$	0.25	21	0.95	79	This work
$Pr_{0.48}Ca_{0.52}MnO_3$	0.21	13	1.36	87	This work
$Pr_{0.6}Ca_{0.4}MnO_3$	0.6	23	2.0	77	[22]
$La_{0.25}Ca_{0.75}MnO_3$	0.67	23	2.3	77	[31]

for $La_{0.50}Ca_{0.50}MnO_3$, $La_{0.48}Ca_{0.52}MnO_3$ and $Pr_{0.48}Ca_{0.52}MnO_3$. This indicates a common origin for the transition in all three materials. However, the amount of entropy released is not correlated with the change in magnetization at the transition (ΔS remains constant, while $\Delta M(La_{0.50}Ca_{0.50}MnO_3) \simeq 10\Delta M(La_{0.48}Ca_{0.52}MnO_3) \simeq 100\Delta M(Pr_{0.48}Ca_{0.52}MnO_3)$). Therefore the mechanism for the transition is independent of the magnetization. Finally, $Pr_{0.48}Ca_{0.52}MnO_3$ has a larger entropy change than $La_{0.48}Ca_{0.52}MnO_3$. $Pr_{0.48}Ca_{0.52}MnO_3$ is also expected to have stronger electron–phonon coupling than $La_{0.48}Ca_{0.52}MnO_3$. Thus the electron–phonon coupling is indicated as the origin of the entropy released at the transitions, as expected for the onset of a CDW. The absence of a detectable thermodynamic effect from the magnetic transition is particularly surprising in $La_{0.50}Ca_{0.50}MnO_3$, in which magnetic effects have long been thought to play an important role in the onset of the superstructure [19, 20].

When passing through a first-order transition, the sample should emit latent heat, producing a PPMS decay curve that cannot be well modelled by the analysis software [32]. Therefore, decay curves were examined in the regions of the transitions, but the values derived manually were the same as the values which had been determined automatically, within experimental error. This absence of latent heat at the transition is the first piece of evidence that the transitions are second order, as would be the case for the onset of a CDW.

The second piece of evidence that the upper transition is second order is that the heat capacity peak is always asymmetric (see figure 2). A second-order transition in a very pure sample can be modelled using critical exponents; however, the breadth of the peak in this case indicated that a model including impurities must be used. We have already noted the similarity of the transitions in the manganites shown in figure 1 to the CDW transition in $Lu_5Rh_4Si_{10}$ [28]. Therefore the heat capacity peak above background at the transition was modelled as a Peierls transition to a CDW state in a system containing impurities [33]:

$$C \propto \frac{\mathrm{d}\chi}{\mathrm{d}t} \propto \frac{\mathrm{d}\kappa_{\mathrm{imp}}}{\mathrm{d}t} \propto \frac{\mathrm{d}}{\mathrm{d}t}\{(-t) + [(-t)^2 + N^4]^{1/2}\}^{1/2} \tag{2}$$

where χ is the magnetic susceptibility, κ_{imp} is the inverse ionic correlation length in the presence of impurities, $N = \Lambda x^{1/d}$ and $t = (T - T^*)/T^*$. Λ is an input lengthscale determined by the impurity potential (taken to be roughly a lattice spacing), d is the system dimension, x is the impurity concentration and $T^* = T_{\mathrm{C}}^{\mathrm{imp}} = T_{\mathrm{C}}^{\mathrm{pure}} - \Delta T$. Since the low and high T limits of this function are not the same, a linear background was subtracted to enable the function to be fitted to the heat capacity above background. The fit can be made over the widest range for $Pr_{0.48}Ca_{0.52}MnO_3$ because the upper transition is well separated from the lower transition. For $La_{0.50}Ca_{0.50}MnO_3$ and $La_{0.48}Ca_{0.52}MnO_3$ the lower transition is close, and therefore the fit must be made over a narrower range. As can be seen from figure 4, the model provides an extremely good fit to the data.

A lengthscale for the disorder was calculated as $x^{-1/d} = \Lambda/N$. For $Pr_{0.48}Ca_{0.52}MnO_3$ and $La_{0.50}Ca_{0.50}MnO_3$ the result was 23 Å, and for $La_{0.48}Ca_{0.52}MnO_3$ it was 21 Å. Therefore the

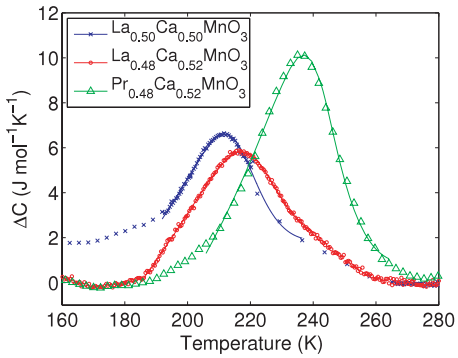

Figure 4. Fitting of transition peaks for $La_{0.50}Ca_{0.50}MnO_3$, $La_{0.48}Ca_{0.52}MnO_3$ and $Pr_{0.48}Ca_{0.52}MnO_3$ to a model of a Peierls transition in a system with impurities (a linear background was removed). Points are data and the solid line is the fit of the model to the data.

lengthscale of the disorder is very similar in all three compounds. By comparison, blue bronze (a charge-density-wave system) doped with 1% W ($K_{0.3}Mo_{0.99}W_{0.01}O_3$) yields a lengthscale of 51 Å. The fact that this model can fit all three compounds, with similar disorder lengthscales, supports the conjecture that the transition is a Peierls transition to a CDW state in disordered materials. The disorder cannot be due to grain boundary effects, since TEM images of these materials show grains of around 2 μm [16, 17]. We suggest that the 'impurities' may in fact reflect the A-site cation inhomogeneity rather than chemical inhomogeneities since x-ray and neutron data indicate that the samples are single phase [17, 25]. Since the level of disorder should be linked to the number of Re/Ae ion size mismatches, one would expect the disorder parameter to be very similar for all three compounds, in agreement with the values above.

In conclusion, our data showed that the upper transition which has been traditionally associated with the onset of FM in $x = 0.5$ is in fact driven by the formation of a CDW. The transition is second order, and can be well modelled as a Peierls transition in a disordered material. The previous conclusion that the transition was first order was based merely on hysteresis in the resistivity data [21], rather than on the measurement of any thermodynamic quantity. Such hysteresis can be explained as being due to lossy kinetics in a CDW-like ground state with disorder [34]. Other work assumes this transition is first order [20], since the electron–phonon coupling is taken to be large. As we have shown, the electron–lattice effects are involved, but the stripe phase can be well modelled as a CDW in which insulating behaviour can be produced without the need to invoke *strong* electron–phonon coupling. This adds to the growing body of evidence that the stripe and FM phases are much more similar than previously thought [35], and indicates that the colossal magnetoresistance present in manganites is driven by the delicate balance between the FM and stripe phase [18].

We thank N D Mathur and N Harrison for helpful comments. Work at NHMFL is performed under the auspices of the NSF, DoE and State of Florida. Work at Cambridge was funded by EPSRC and the Royal Society. S Cox acknowledges support from the Seaborg Institute.

References

[1] Chen C H *et al* 1997 *J. Appl. Phys.* **81** 4326
[2] Mori S *et al* 1998 *Nature* **392** 473
[3] Tranquada J M *et al* 1995 *Nature* **375** 561

[4] Chen C H *et al* 1993 *Phys. Rev. Lett.* **71** 2461
[5] Vogt T *et al* 2000 *Phys. Rev. Lett.* **84** 2969
[6] Chen C H and Cheong S-W 1996 *Phys. Rev. Lett.* **76** 4042
[7] Radaelli P G *et al* 1997 *Phys. Rev.* B **55** 3015
[8] Radaelli P G *et al* 1999 *Phys. Rev.* B **59** 14440
[9] Wang R *et al* 2000 *Phys. Rev.* B **61** 11946
[10] Nagai T *et al* 2003 *Phys. Rev.* B **68** 092405
[11] Rodriguez-Carvajal J *et al* 2002 *Physica* B **320** 1
[12] Daoud-Aladine A *et al* 2002 *Phys. Rev. Lett.* **89** 097205
[13] Rodriguez E E *et al* 2005 *Phys. Rev.* B **71** 104430
[14] Goff R J and Attfield J P 2004 *Phys. Rev.* B **70** R140404
[15] Subias G *et al* 1997 *Phys. Rev.* B **56** 8183
[16] Loudon J C *et al* 2005 *Phys. Rev. Lett.* **94** 097202
[17] Cox S *et al* 2006 *Preprint* cond-mat/0704.2598
[18] Milward G C *et al* 2005 *Nature* **433** 607
[19] Ramirez A P *et al* 1996 *Phys. Rev. Lett.* **76** 3188
[20] Ramirez A P, Cheong S-W and Schiffer P 1997 *J. Appl. Phys.* **81** 5337
[21] Fernandez-Diaz M T *et al* 1999 *Phys. Rev.* B **59** 1277
[22] Lees M R *et al* 1999 *Phys. Rev.* B **59** 1298
[23] Loudon J C *et al* 2005 *Phil. Mag.* **85** 999
[24] Shannon R D 1976 *Acta Crystallogr.* A **32** 751
[25] Williams A J *et al* 2003 *J. Sol. State Chem.* **173** 456
[26] Grüner G 1994 *Density Waves in Solids* (Reading, MA: Addison-Wesley)
[27] Huber P J 1981 *Robust Statistics* (New York: Wiley)
[28] Lue C S *et al* 2002 *Phys. Rev.* B **66** 033101
[29] Cheong S-W and Hwang H Y 2000 *Colossal Magnetoresistive Oxides* ed Y Tokura (London: Gordon and Breach) pp 237–80
[30] Loram J 2005 private communication
[31] Zheng R K *et al* 2003 *J. Appl. Phys.* **94** 514
[32] Lashley J C *et al* 2003 *Cryogenics* **43** 369
[33] Chandra P 1989 *J. Phys.: Condens. Matter* **1** 10067
[34] Lue C S *et al* 2002 *Phys. Rev.* B **66** 033101
[35] Mannella N *et al* 2005 *Nature* **438** 474